

An Investigation of Maple Wood Baseball Bat Durability as a Function of Bat Profile using LS-DYNA[®]

Blake Campshure, Patrick Drane, James Sherwood
Department of Mechanical Engineering, University of Massachusetts Lowell
One University Ave. Lowell, MA. 01854, USA

Abstract

*During the 2008 Major League Baseball (MLB) season, there was a perception that the rate at which wood bats were breaking was increasing. MLB responded by implementing changes to the wood bat regulations that were essentially transparent to the players, e.g. changing the orientation for the hitting surface on maple bats, setting a lower bound on wood density, and reducing the allowable range for the slope of grain (SoG) of the wood used to make bats. These new regulations resulted in a 65% reduction in the wood-bat breakage rate. It is proposed that a further reduction can be realized by accounting for the role that bat profile plays with respect to bat durability. To begin to develop an understanding of this relationship, a parametric study was conducted using a finite element model on three baseball bat profiles made from maple wood. These bat profiles that span a range of volumes were examined using LS-DYNA to observe their response to bat/ball impacts over a range of game-like speeds. The Altair HyperMesh and LS-PrePost[®] pre-processors were used in the making of the geometric representation and finite element meshing of the models. The mechanical behavior of the maple wood and its fracturing were modeled using the *MAT_WOOD material model in combination with the *MAT_ADD_EROSION option, respectively. The effective wood material properties were varied as a function of wood density. Results include how bat profile and SoG influence bat durability, where durability is defined as the relative bat/ball speed that results in crack initiation, i.e. the higher the breaking speed, the better the durability. The effective durability of the bat as a function of profile was found to be well predicted by the LS-DYNA modeling.*

Introduction

Historically, professional baseball games use wooden baseball bats, which can be classified to break in one of two modes: single-piece failure (SPF) and multi-piece failure (MPF). In response to a perceived increased rate of MPFs in baseball games, Major League Baseball (MLB), issued changes to the Wooden Baseball Bat Specifications (WBBS) which set a required range for allowable Slope of Grain (SoG) in the wood used to manufacture professional baseball bats, as well as instituted inspections by a third party of the bats [1]. Traditionally, any species of wood could be used in a MLB game but changes to the WBBS for the 2010, 2011, and 2012 seasons specified allowable wood species and gradually increased the lower bound of wood density used in professional bats [2-5]. In turn, this increase in the minimum allowable density would increase the minimum breaking strength of the wood. These changes led to a 65% reduction in MPF rate [6].

It is believed that a further reduction in the MPF rate can be realized by also considering the role that bat profile has with respect to bat durability. Previous work has outlined a finite element modeling approach and shown that SoG and bat taper geometry independently influence baseball bat durability [7-9]. The aim of the current work is to conduct a parametric study to understand how the combination of SoG and bat profile influences bat durability.

Methodology

Bat Profiles

The four major regions of a baseball bat profile, i.e. shape, are shown in Figure 1. The knob is a register point for the hands and helps to keep the bat in the player’s hands during the swing. The handle is where the player grips the bat and is the thinnest part of the bat. The taper region transitions the handle to the barrel. The player hits the baseball with the barrel portion of the bat, which is the thickest section of the baseball bat. Depending on a player’s desired handle, barrel length, and diameter, the taper can vary significantly from profile to profile.

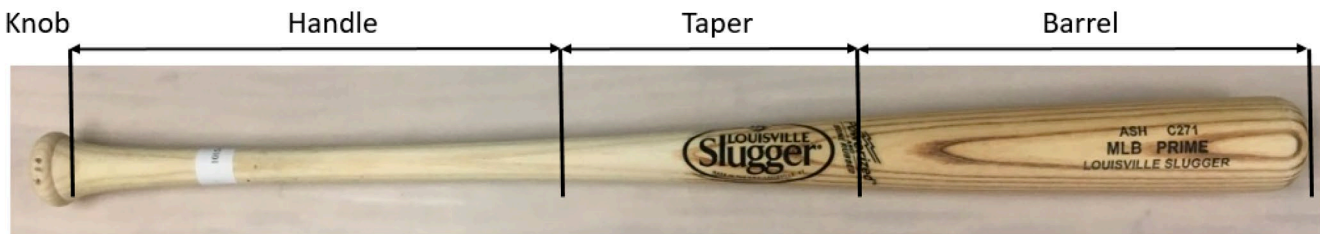





Figure 1: The four section of a baseball bat.

For this investigation, three bat profiles that have varying geometries and volumes were selected. Table 1 shows bat diameter measurements for each of the three profiles at specific axial locations of interest. These locations are measured from the knob end of the bat. Of the three profiles, Bat Profile A has the largest handle, barrel and the largest diameters at the 12 in. (30.5 cm), 16.5 in. (41.9 cm), 18 in. (45.7 cm), and 21 in. (53.3 cm.) locations as measured from the base of the knob. At the 18 in. (45.7 cm.) and the 21 in. (53.3 cm.) locations, Bat Profile A has the largest measurements, which indicates that it has the longest handle of the three bat profiles. Bat Profile C has the median diameter of the three for the handle up to the 21-in. (53.3-cm) location but the smallest maximum barrel diameter, which suggests it has the most gradual diameter change through its taper region. Lastly, Bat Profile B has the smallest minimum handle diameter but has the median diameter of the three profiles for the 21-in. (53.3-cm) location through the barrel.

Table 1: Bat Profile Geometric Comparison

Profile ID	Profile Image	Minimum Handle Diameter in. (cm.)	12in. (30.5 cm) Location in. (cm.)	16.5in. (41.9 cm) Location in. (cm.)	18 in. (45.7 cm.) Location in. (cm.)	21 in. (53.3 cm) Location in. (cm.)	Maximum Barrel Diameter in. (cm.)
A		0.99 (2.52)	1.13 (2.88)	1.39 (3.52)	1.56 (3.95)	2.03 (5.14)	2.65 (6.74)
B		0.93 (2.36)	1.08 (2.75)	1.32 (3.35)	1.48 (3.75)	1.93 (4.90)	2.56 (6.50)
C		0.96 (2.43)	1.07 (2.71)	1.37 (3.48)	1.49 (3.78)	1.85 (4.70)	2.52 (6.40)

Finite Element Modeling

The geometry and meshing of the finite element models were created using Altair HyperMesh (Altair Engineering, Inc. Troy, MI, USA). The models were created to replicate the ADC durability setup at the University of Massachusetts Lowell (UML, Lowell, MA) and consist of a baseball bat resting between sets of rubber rollers attached to a rotating plate and a baseball. Figure 2 shows the model in HyperMesh compared to the ADC durability machine at UML. The pairs of compliant rollers represent a player’s grip on the baseball field [10].

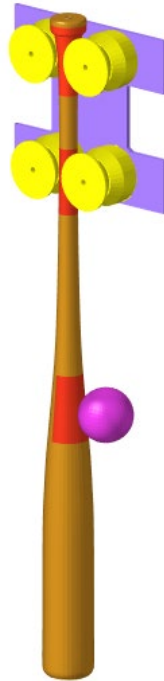


Figure 2: Hypermesh model of baseball bat.

All finite element analyses were completed using LS-DYNA (Livermore Software Technology Corporation, Livermore, CA, USA). Each baseball bat model was constructed of 8-noded brick elements with single-point integration. The `*CONTACT_SURFACE_TO_SURFACE` keycard was utilized to define five contacts. Contact was defined between the baseball bat and the baseball and the remaining four contacts between the bat and the rollers were defined. The `*MAT_WOOD` (material model #143) was used to represent the maple wood. The mechanical properties of the maple wood used in the bat models are reported by Fortin-Smith *et al.* [11]. They are shown in Table 2. Each bat profile was to maintain a weight of 31 oz. (879 g), but the geometry differences among the volumes of respective bat profiles resulted in a variation in the density of the wood used in each finite element model. The mechanical and strain-to-failure properties of the maple wood are a function of the density, which is why they vary between the respective profiles. `*MAT_ELASTIC` (Material Model #001) was used to represent the rubber rollers and `*MAT_VISCOELASTIC` (Material Model #006) was used to model the baseball.

A strain-to-failure criterion was chosen to capture crack initiation and propagation in the finite element models. To accomplish wood cracking as a function of strain, the `*MAT_ADD_EROSION` keycard was utilized. This option allowed for element elimination once an element reached a maximum principle strain value. Strain-to-failure properties have been found to be a function of density. The values used in the finite element models are shown in Table 2. To simulate SoG of the maple wood, the AOPT option of the `*MAT_WOOD` material was activated. Because the elements of the baseball bat models were solid elements, the AOPT option was set to 2. The AOPT option defines a local coordinate system for the maple wood material. To assign local material coordinates to the maple wood material, two vectors need to be input to the AOPT boxes on the `*MAT_WOOD` keycard. Vector A is given as an input for the 1-direction of the material, while Vector D is given as an input for the 2-direction of the solid wood material. In the bat models, the 1-direction runs down the length of the baseball bat and the 2-direction is perpendicular to the 1-direction. Both Vector A and Vector D of the AOPT option are input as components of the global coordinate system using direction cosines. This option is more convenient than inputting the mechanical properties as a component of SoG. Among the models of one bat profile, all the mechanical properties remained constant while the AOPT vectors varied with respect to SoG.

Each of the three bat profiles were given SoGs between ±10° to investigate the relationship between bat profile and bat durability.

Lastly, the bat models were constrained at the corner nodes to prevent translation in the X, Y, and Z-directions but are still able to rotate. The *INITIAL_VELOCITY_NODE keyword card was used to prescribe a desired velocity to all of the nodes of the baseball.

Table 2: Wood Mechanical Properties used in Baseball Bat Finite Element Models.

Material Property	LS-DYNA Material Variable	Unit	Bat Profile A		Bat Profile B		Bat Profile C	
Volume	-	in ³ (cm ³)	88.657	(1453)	84.24	(1380)	79.684	(1305)
Density	RO	lb/in ³ (g/cm ³)	0.0219	(0.606)	0.023	(0.637)	0.0243	(0.673)
Strain-To-Failure	MAXEPS	-	0.0212		0.0223		0.0234	
Parallel Normal Modulus	EL	psi (GPa)	2,152,281	(14.8)	2,198,071	(15.2)	2,250,619	(15.5)
Perpendicular Normal Modulus	ET	psi (GPa)	139,898	(0.97)	142,875	(0.99)	146,290	(1.01)
Parallel Shear Modulus	GLT	psi (GPa)	238,903	(1.65)	243,986	(1.68)	249,819	(1.72)
Perpendicular Shear Modulus	GTR	psi (GPa)	76,192	(0.52)	77,813	(0.54)	79,673	(0.55)
Poisson's Ratio	PR	-	0.476		0.476		0.476	
Parallel Tensile Strength	XT	psi (Mpa)	19,358	(133.5)	20,507	(141.4)	21,826	(150.5)
Parallel Compressive Strength	XC	psi (Mpa)	9,654	(66.6)	10,227	(70.5)	10,884	(75.0)
Perpendicular Tensile Strength	YT	psi (Mpa)	1,861	(12.8)	1,971	(13.6)	2,097	(14.5)
Perpendicular Compressive Strength	YC	psi (Mpa)	1,812	(12.5)	1,920	(13.2)	2,044	(14.1)
Parallel Shear Strength	SXY	psi (Mpa)	2,873	(19.8)	3,043	(21.0)	3,239	(22.3)
Perpendicular Shear Strength	SYZ	psi (Mpa)	4,022	(27.7)	4,261	(29.4)	4,535	(31.3)

Post-processing was conducted in LS-PrePost (Livermore Software Technology Corporation, Livermore, CA, USA). The finite element models were analyzed for a range of baseball impact velocities from 90 mph (145 km/h) to 180 mph (290 km/h) in 5 mph (km/h) increments. In the finite element models, there are three possible outcomes for the bat/ball impact, i.e. no failure (NF), single-piece failure (SPF), and multi-piece failure (MPF). NF occurs if there is no crack initiation after bat/ball impact. SPF occurs when the bat cracks but stays relatively intact. MPF occurs when the bat breaks into multiple large pieces, where a large piece is defined as a chunk of the bat that weighs 1.00 oz. (28.4 g) or more. Figure 3 shows an example of each of the possible outcomes for the finite element model. Figure 4 shows the three possible outcomes as observed in testing at UML.

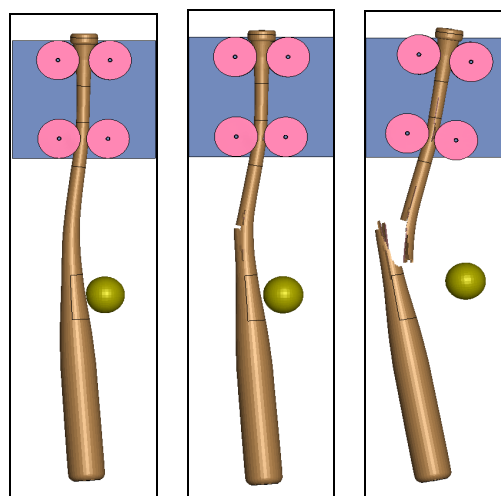


Figure 3: Three possible outcomes of the finite element analyses: No Failure (Left), Single-Piece Failure (Middle), and Multi-Piece Failure (Right).

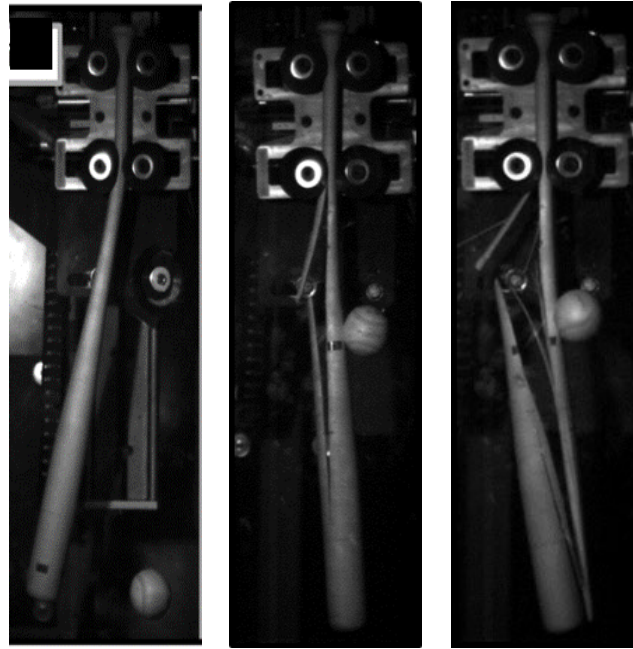


Figure 4: Three possible outcomes of the bat/ball impact as observed in testing at UML: No Failure (Left), Single-Piece Failure (Middle), Multi-Piece Failure (Right)

Two ball-impact locations were studied in this investigation, i.e. 2.0 in. (5.1 cm) and 14.0 in. (35.6 cm) as measured from the barrel end of the baseball bat. These two impact locations are positioned away from the first and second nodes of bending, which lead to large-amplitude vibrations along the length of the bat. They have also been observed to be critical ball impact locations for MPF breakage in professional baseball games.

The range of prescribed ball velocities originally spanned from 90-180 mph (145-290 km/h). The 14.0 in. (35.6 cm) impact location velocities ranged from 90 to 145 mph (145-233 km/h), which corresponds to a 60-100% maximum velocity assuming a 90 mph (145 km/h) pitch and a 90 mph (145 km/h) swing velocity rotating about an axis that is 6 in. (15.2 cm) from the base of the knob. Using the same logic, the ball impact velocity range for the 2.0 in. (5.1 cm) impact location increased the velocity up to 180 mph (233 km/h). Following the finite element analyses of the original impact velocity range, it was determined that this range needed to be expanded to capture the NF to SPF and SPF to MPF threshold velocities. The velocity range was increased to 70-210 mph (113-322 km/h). In total, 1551 combinations of bat profile, ball impact velocity, impact location and SoG were analyzed using LS-DYNA.

Results

The results of the finite element models were analyzed to understand how durability changes as a function of bat geometry (profile) and SoG. Table 3 summarizes the peak velocities resulting in NF (the NF to SPF threshold velocity) and SPF (the SPF to MPF threshold velocity) as a function of bat profile and SoG. For each of the three examined baseball bat profiles, contour plots depicting the three outcomes as a function of ball impact velocity and SoG were constructed. The contour plots are shown in Figure 5. Each color shown on the contour plots corresponds to one of the three possible outcomes for each ball impact velocity, SoG and bat profile: i.e. NF, SPF, and MPF. Green, yellow, and red are associated with NF, SPF and MPF, respectively. The dashed vertical lines denote the positive and negative SoG bounds in compliance with the MLB allowable $\pm 3^\circ$ SoG. The solid vertical line denotes the 0° SoG condition.

Table 3: Peak Impact Velocities and SoG associated with NF and SPF outcomes

Bat Profile	NF to SPF Transition				SPF to MPF Transition			
	14.0 in. (35.6 cm) Impact		2.0 in. (5.1 cm) Impact		14.0 in. (35.6 cm) Impact		2.0 in. (5.1 cm) Impact	
	Speed (mph) [km/h]	SoG (deg)	Speed (mph) [km/h]	SoG (deg)	Speed (mph) [km/h]	SoG (deg)	Speed (mph) [km/h]	SoG (deg)
A	135 [217]	2	130 [209]	0	155 [249]	0	180 [290]	-1
B	120 [193]	2	125 [201]	0	160 [257]	0	175 [282]	-1
C	130 [209]	2	140 [225]	0	160 [257]	0	160 [258]	0

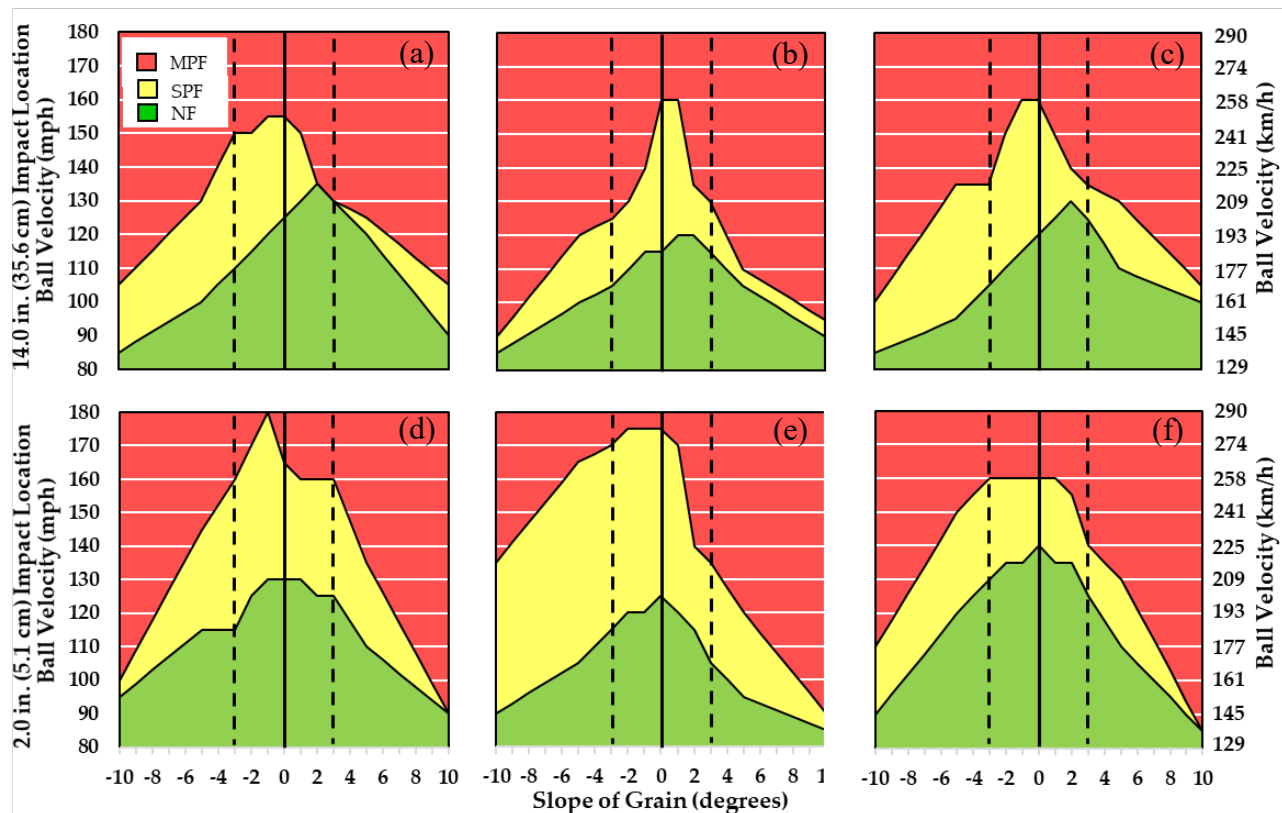


Figure 5: Top Row, left to right– 14.0 in. (35.6 cm) impact models for (a) Profile A, (b) Profile B, and (c) Profile C, respectively. Bottom Row, left to right– 2.0 in. (5.1 cm) impact models for (d) Profile A, (e) Profile B, and (f) Profile C, respectively.

Discussion

The information in Table 3 shows the maximum NF to SPF threshold velocities and SPF to MPF threshold velocities for all three of the bat profiles, and Figure 5 illustrates the outcomes of the finite element models with respect to ball impact location, ball impact velocity, SoG, and bat profile. Maximum threshold velocities for the (outside-pitch) 2.0 in. (5.1 cm) occur at -1° SoG for NF outcome and 0° SoG for SPF outcome for all three of the bat profiles. Maximum threshold velocities for the (inside-pitch) 14.0 in. (35.6 cm) impact location occur at +2° SoG for NF outcome and 0° SoG for SPF outcome. During post processing, it was observed that the inside- and outside-pitch impact locations created different crack initiation sites. The 2.0-in. (5.1-cm) impact location created crack initiation near the roller support on the impact-side of the baseball bat, which is analogous in beam-theory to the cracking on the tensile surface of a tip-loaded cantilever beam. The 14.0-in. (35.6-cm)

impact location created crack initiation in the taper region on the side opposite of the baseball impact, which is analogous in beam-theory to the cracking on the tensile surface of a beam that is clamped at one end and pin-supported on the other end with a mid-span point load.

When analyzing Figure 5 closely, it is observed that the durability of Bat Profile B is more dependent on SoG than the other bat profiles even though it still has one of the highest SPF to MPF threshold velocities. Conversely, Bat Profile A has a much flatter SPF to MPF threshold velocity from -3° to $+1^\circ$ SoG, which suggests that the durability of Bat Profile A has the lowest dependency on SoG of the three profiles. At the 2.0-in (5.1-cm) impact location, the durability of Bat Profile C shows the lowest influence of SoG due to the flatness of its SPF to MPF threshold velocity curve. Lastly, it was observed that all of the plots are asymmetric about their respective peaks. It can be seen in the contour plots that there is a large drop in bat durability as the SoG progresses in the positive direction away from the SPF to MPF threshold velocity compared to the same progression in the negative direction.

Overall, the differences in the curve of the SPF to MPF between the bat profiles and the asymmetry of the curves suggest that the geometry of the baseball bat has an impact on bat durability with respect to slope of grain. Among the three bat profiles examined in this work, there is a tendency for the optimal SoG range to be from -3° to $+1^\circ$.

Conclusions

In the current work, three different baseball bat profiles were analyzed using LS-DYNA to understand how baseball bat durability changes with respect to baseball bat profile, impact location and SoG. The mechanical behavior of the maple wood of the baseball bats was captured using the *MAT_WOOD material model. To accommodate crack initiation and propagation, the *MAT_ADD_EROSION material model option with a strain-to-failure criterion was used in conjunction with the *MAT_WOOD material model. Finally, the AOPT option was set to 2 in the *MAT_WOOD keycard to create a local coordinate system of the maple wood, which created a SoG of the material. The results of the finite element models show that bat durability is a function of the combination of bat profile and SoG.

References

1. Major League Baseball, 2008. Major League Baseball 2009 Bat Supplier Regulations, The Office of the Commissioner of Baseball. December 15.
2. Major League Baseball, 2010a. Major League Baseball 2010 Bat Supplier Regulations, The Office of the Commissioner of Baseball. January 6th.
3. Major League Baseball, 2010b. Agreement regarding Players' use of approved bats in Major League games for the 2010 season. The Office of the Commissioner of Baseball. January 7th.
4. Major League Baseball, 2011c. Major League Baseball 2011 Bat Supplier Regulations, The Office of the Commissioner of baseball.
5. Major League Baseball, 2012d Major League Baseball 2012 Bat Supplier Regulations, The Office of the Commissioner of Baseball. December
6. Saraceno, J. Taking swing at safer bats, man says his creation curbs exploding effect. *USA TODAY*, FA CHASE EDITION P.1C 15 August 2016.
7. Fortin-Smith J., Sherwood J., Drane P., and Kretschmann D. 2016. "A Complementary Experimental and Modeling Approach for the Characterization of Maple and Ash Wood Material Properties for the Bat/Ball Impact Modeling in LS-DYNA." 14th *International LS-DYNA Users Conference*, June12-14, 2016. Dearborn, MI.

8. Fortin-Smith, J.; Sherwood, J.; Drane, P.; Ruggiero, E.; Campshure, B.; Kretschmann, D. A Finite Element Investigation into the Effect of Slope of Grain on Wood Baseball Bat Durability. *Applied Sciences* **2019**, *9*, 3733.
9. Fortin-Smith J., Sherwood J., Drane P., and Kretschmann D. 2016. "An Investigation into the Relationship between Wood Bat Durability and Bat Taper Geometry using LS-DYNA." *14th International LS-DYNA Users Conference, June 12-14, 2016*. Dearborn, MI.
10. Drane, P.; Sherwood, J.; Shaw, R. An Experimental Investigation of Baseball Bat Durability. In the Engineering of Sport 6; Moritz, E.F., Haake, S., Eds.; Springer: New York, NY, USA, 2006
11. Fortin-Smith, J.; Sherwood, J.; Drane, P.; Kretschmann, D. Characterization of Maple and Ash Material Properties for the Finite Element Modeling of Wood Baseball Bats. *Applied Sciences* **2018**, *8*, 2256